



# Monte Carlo simulation of thermophysical properties of liquid Ni-15%X (Co, Cu, Yb) alloys

Wenjin Chen<sup>1</sup> · Wenjing Yao<sup>1</sup> · Ding Wang<sup>2</sup> · Weigang Zhang<sup>2</sup>

Received: 9 November 2019 / Accepted: 9 January 2020 / Published online: 31 January 2020  
© Springer-Verlag GmbH Germany, part of Springer Nature 2020

## Abstract

In this paper, the embedded-atom method was used to study the influence of different solute elements (Co, Cu, Yb) on the thermophysical properties of liquid Ni-based alloys. By exploring the relationship between surface tension, viscosity, diffusion coefficient and temperature of liquid Ni-based alloys with three solutes in the range of 1500~1900 K, we found that under certain components the surface tension of liquid Ni-based alloys with three solutes decreased as temperature increased. Except the case that the atomic radius of the same period decreased with the increase of the atomic number and influence of lanthanide and actinide contraction, the surface tension of liquid Ni-based alloys decreased with the increase of atomic number. The viscosity of liquid alloy showed a downward trend with increasing temperature, and the viscosity decreased exponentially with the temperature increasing under certain components. The variation trend of diffusion coefficient of the three kinds of atoms was similar to that of the temperature, which increased with the increase of temperature under the same component. Especially, the diffusion coefficient increases exponentially with the increase of temperature under certain components. These simulated data provided necessary thermophysical parameters for non-equilibrium dynamics analysis of liquid-phase alloys and also supplied a sound theoretical basis for exploring the internal physical mechanism of “liquid microstructures–thermophysical properties–preferred phase of nucleation”.

**Keywords** Monte Carlo simulation · The embedded-atom method · Thermophysical properties · Ni-based alloys

## 1 Introduction

Ni-based alloys are the most widely used superalloy materials, but in the actual process of production, the processing technology of superalloy is complicated and the control requirements are high, resulting in high experimental cost and long research and development cycle. With the continuous improvement of computer software and hardware performance, numerical simulation technology has been developing rapidly and is widely used in guiding the practice of industrial production [1, 2]. It is helpful in simulating the solidification process, predicting morphologies and defects, and optimizing the production process, while shortening the time and costs of research [3–6]. At present, the experimental conditions for measuring high temperature liquid metals

as well as supercooled metals are difficult. Therefore, molecular simulation methods as a useful method are applied to calculate the thermophysical properties of many kinds of liquid metals [7–10]. Thermophysical properties of liquid metal have an important influence on liquid–solid phase transition behavior, crystallization and grain growth process [4]. The surface tension of liquid metal is one of the most basic physical properties for understanding the metallurgical process. The temperature coefficient of surface tension is the key parameter in the preparation of high-performance metal materials under space conditions [11]. In the metal smelting and refining process, surface and interfacial tension is a controlling factor for many metallurgical phenomena [12–15], such as gas absorption, bubble nucleation, nucleation and growth of non-metallic inclusions, etc. Therefore, the determination and prediction of surface tension and temperature coefficient of liquid metals have been an important part in the study of the thermophysical properties of metals and metallurgical research.

This paper discusses the thermophysical properties of Ni-15%X (Co, Cu, Yb) alloys by means of Monte Carlo method.

✉ Weigang Zhang  
laverne1118@126.com

<sup>1</sup> Northwestern Polytechnical University, Xi'an 710129, China

<sup>2</sup> Western Metal Materials CO., LTD, Xi'an 710201, China

The dependence of surface tension, viscosity and diffusion coefficient of liquid metals on the temperature is obtained by calculating the surface tension at different temperatures. Finally, the effects of three elements on the thermophysical properties of Ni alloys are summarized and analyzed by combining the simulated data and the available experimental results. These results provide a reference for the preparation of new Ni-based alloys, and also supply a theoretical basis for the study of the relationship between thermophysical properties and microstructure of Ni–Co, Ni–Cu and Ni–Yb liquid alloys.

## 2 Simulation methods and calculation principle

### 2.1 Configuration initialization of system

Monte Carlo simulation is performed in Canonical ensemble (NVT ensemble), Ni-15%X (Co, Cu, Yb) system which is composed of 864 atoms of face-centered cube, in the primitive cell (0, 0, 0), (a<sub>0</sub>/2, 0, a<sub>0</sub>/2), (a<sub>0</sub>/2, a<sub>0</sub>/2, 0), (0, a<sub>0</sub>/2, a<sub>0</sub>/2) four points as a benchmark, a<sub>0</sub> is the crystal constant derived from the density of liquid alloy, the periodic boundary condition. The analytic embedded-atom method is adopted and then the corresponding number of Ni atoms in the system are replaced by Co, Cu, Yb to complete the structure initialization.

A definite temperature *T* is selected near the melting point and the total energy of the system at this temperature is obtained [16, 17]:

$$E_{\text{tot}} = NE, \tag{1}$$

$$E = F(\rho) + \frac{1}{2} \sum_m \phi(r_m), \tag{2}$$

$$\rho = \sum_m f(r_m), \tag{3}$$

where *F* is the embedding energy of the atoms embedded in the electron cloud density at  $\rho$ ,  $\phi$  is a short-range interaction potential between the *i* atom and the *j* atom (the repulsive potential between the atoms), *r<sub>m</sub>* is the distance between the atom *i* and the atom *j*,  $\rho$  is the electron cloud density, and *f*(*r<sub>m</sub>*) is the attraction potential between the outermost electrons of the two atoms.

For a binary system, the size of the system is bound to be related to the repulsive potential of the homogeneous atoms and the mole ratio of each atom. Therefore, it is necessary to make linear superposition of repulsive potentials between different kinds of atoms [18].

$$\phi^{ab}(r) = \frac{1}{2} \left[ \frac{f^b(r)}{f^a(r)} \phi^{aa}(r) + \frac{f^b(r)}{f^a(r)} \phi^{bb}(r) \right]. \tag{4}$$

The system energy of the ideal lattice can be expressed as

$$E(r_1) = F(\rho(r_1)) + \varphi(r_1), \tag{5}$$

$$\phi(r_1) = \frac{1}{2} \sum_m \varphi(r_m). \tag{6}$$

Rose et al. proposed the energy equation of solids [19]:

$$E(r_1) = -E_C \left[ 1 + \alpha \left( \frac{r_1}{r_{1\epsilon}} - 1 \right) \right] \exp \left[ -\alpha \left( \frac{r_1}{r_{1\epsilon}} - 1 \right) \right], \tag{7}$$

where  $\alpha = \sqrt[3]{\frac{\Omega_e B_e}{E_C}}$ ,  $\Omega_e$  is the atomic volume, *B<sub>e</sub>* is the bulk modulus, *r<sub>1ε</sub>* is the nearest neighbor spacing at equilibrium state, *E<sub>C</sub>* is the cohesive energy, and cutoff radius of potential function *r<sub>1</sub>* = 3 × *r<sub>1ε</sub>*. Thus, the embedding energy can be expressed as

$$F(r_1) = -E_C \left[ 1 + \alpha \left( \frac{r_1}{r_{1\epsilon}} - 1 \right) \right] \exp \left[ -\alpha \left( \frac{r_1}{r_{1\epsilon}} - 1 \right) \right] - \phi(r_1). \tag{8}$$

For the intact FCC crystal, if we only consider the contribution of the nearest neighbor atoms to the electron density and the double potential.

$$\rho(r_1) = 12f(r_1), \tag{9}$$

$$\phi(r_1) = \frac{1}{2} \sum_m \phi(r_m). \tag{10}$$

Let the electron density function and the ion pair of the potential function take the following form:

$$\rho(r) = \rho_e \exp \left[ -\beta \frac{r_1}{r_{1e}} - 1 \right], \tag{11}$$

$$f(r) = f_e \exp \left[ -\beta \left( \frac{r_1}{r_{1e}} - 1 \right) \right] \quad r \leq r_c. \tag{12}$$

Therefore, the embedded energy Eq. (8) can be written as a function of electron density.

$$F(\rho) = -E_C \left( 1 - \frac{\alpha}{\beta} \ln \frac{\rho}{\rho_e} \right) \left( \frac{\rho}{\rho_e} \right)^{\alpha/\beta} - \phi \left( \frac{\rho}{\rho_e} \right)^{\gamma/\beta}, \tag{13}$$

where  $\rho_e = 12 f_e$ ,  $\Phi = 6 \phi_e$ ,  $\beta$  is the slope of the electron density at the nearest neighbor spacing,  $E_{1v}^{UF} = -12F(\rho_e) + 12F(\frac{11}{12}\rho_e) - \phi_e$ , and it is obtained by fitting with energy generated by the unsagging hole.

And those for Yb atom are [20]:

$$f_j^c(r) = f_e \frac{r}{r_{1e}} \exp \left[ -\beta \left( \frac{r}{r_{1e}} - 1 \right) \right], \tag{14}$$

$$\phi^{cc}(r) = -\phi_e \left[ 1 + \delta \left( \frac{r}{r_{1e}} - 1 \right) \right] \exp \left[ -\lambda \left( \frac{r}{r_{1e}} - 1 \right) \right], \tag{15}$$

$$F(\rho) = -F_0 \left[ 1 - n \ln \left( \frac{\rho}{\rho_e} \right) \right] \left( \frac{\rho}{\rho_e} \right)^n. \tag{16}$$

Here,  $r_{1e}$  is the nearest neighbor spacing at equilibrium state, and  $\delta$ ,  $\lambda$  and  $\beta$  are model parameters.

### 2.2 Acquisition method of thermophysical properties

The simulated system is a rectangular cube with periodic boundary condition, and the cohesive work can be calculated by calculating the interaction between different side atoms, which is equal to two times the specific surface free energy [21].

$$\sigma = \frac{W}{2S}. \tag{17}$$

I. Egry pointed out that the surface tension and viscosity of liquid metal have the following relationship [22]:

$$\eta = \frac{16}{15} \sqrt{\frac{M}{kT}} \sigma. \tag{18}$$

The diffusion coefficient can be calculated by the Stokes–Einstein formula [23]:

$$D = \frac{kT}{4\pi r \eta}, \tag{19}$$

where  $M$  is absolute atomic mass according to the compositions of the system and  $k$  is the Boltzmann constant. According to the law of viscosity and diffusion coefficient,  $\eta_0$ ,  $Q_\eta$ ,  $D_0$ ,  $Q_d$  can be fitted, where  $R$  is the universal gas constant,  $Q_\eta$  is the apparent activation energy, and  $Q_d$  is the diffusion activation energy.

$$\eta = \eta_0 \exp \frac{Q_\eta}{RT}, \tag{20}$$

$$D = D_0 \exp \left( -\frac{Q_d}{RT} \right). \tag{21}$$

For the heating process of a constant pressure system, the specific heat is the fluctuation of the system energy with temperature. Previous studies have shown that the specific heat of liquid metal increases gradually with decreasing

temperature, assuming that specific heat is linearly related to temperature [24–26].

$$C_P(T) = \frac{dE(T)}{dT}, \tag{22}$$

$$C_P(T) = C_{P_0} + \frac{dC_P}{dT} (T - T_m). \tag{23}$$

$C_{P_0}$  is the specific heat at the corresponding melting point temperature,  $dC_P/dT$  is the temperature coefficient of specific heat, and  $T_m$  is the melting point. Hence, the system energy is the quadratic function of temperature in constant pressure heating process.

$$E(T) = E_0 + \left( C_{P_0} - \frac{dC_P}{dT} \cdot T_m \right) T + \frac{1}{2} \frac{dC_P}{dT} T^2. \tag{24}$$

As a result, by simulating the energy of the system at each temperature and performing the energy quadratic function fitting, we get the fitting equation as follows  $E(T) = A_0 + A_1 T + A_2 T^2$ , and the specific heat and specific heat coefficient of the simulated object are obtained at its melting point temperature.

## 3 Simulation results and analysis

### 3.1 Simulation results and analysis of surface tension and its temperature coefficient

The surface tension of Ni-15%X (Co, Cu, Yb) at different temperatures and its linear fitting results are obtained by simulation. As shown in Fig. 1, the functional relationship

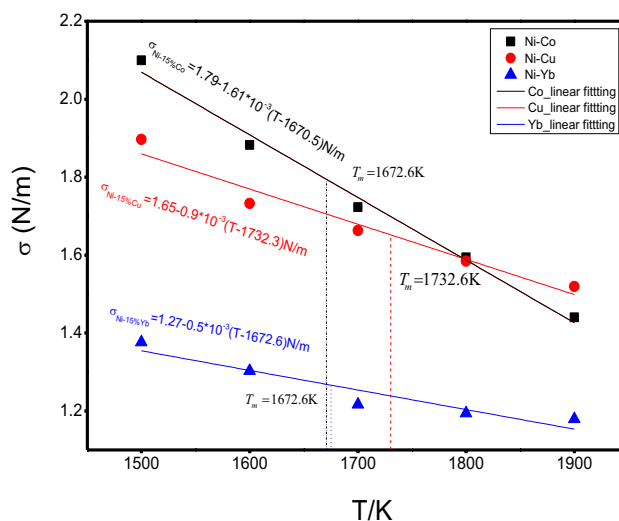


Fig. 1 The fitting results of surface tension of liquid Ni-15%X (Cu, Co, Yb) alloys with temperature

between the surface tension of liquid Ni-based alloys with different solutes and temperature can be obtained. Therefore, we calculated the qualitative effects of the temperature coefficient of the surface tension and different atomic number atoms as the solute elements on thermophysical properties of Ni-based alloys.

The fitting formulas between the surface tension of Ni-based alloys and temperature are as follows:

$$\sigma = \sigma_0 + \frac{d\sigma}{dT}(T - T_m), \quad (25)$$

$$\sigma_{\text{Ni-15\%Co}} = 1.79 - 1.63 \times 10^{-3}(T - 1670.5), \quad (26)$$

$$\sigma_{\text{Ni-15\%Cu}} = 1.65 - 0.90 \times 10^{-3}(T - 1732.3), \quad (27)$$

$$\sigma_{\text{Ni-15\%Yb}} = 1.27 - 0.50 \times 10^{-3}(T - 1672.6), \quad (28)$$

where  $\sigma$  is the surface tension and  $d\sigma/dT$  is the temperature coefficient of surface tension.

The surface tension of liquid Ni-based alloys with three different solutes decreases with the increase of temperature. Under the same component, the surface tension varies linearly with temperature. The simulation results are consistent with the actual situation, and the rise of temperature gives rise to expansion of the system and larger spacing of atoms. In addition, the interaction potential among atoms decreases, and its total surface area increases, which indicate that specific surface energy is reduced. Considering molecular potential energy, the potential energy of surface atoms is higher than that of internal atoms. Hence, the atoms have a tendency to move toward the internal system to reduce the overall energy and thereby reduce the total surface area of the system (Table 1).

At the same temperature, the surface tension of liquid Ni-based alloys decreases gradually as the atomic number of solute elements increases. In the case of those three solute elements, Cu and Co are subgroup element atoms of the same period, where Cu produces 4 s orbitals after hybridization of extranuclear electron. Therefore, the number of layers of extranuclear electron is more than that of Co, resulting in larger atomic radius compared with Co. In contrast, the atomic spacing of Ni–Cu alloy is larger and the interaction potential is weakened, and the total surface area increases, causing the surface tension to decrease. Yb is one of the lanthanide elements. Although its atomic number is far bigger than Cu and Co, the atomic radius is the same. The same analysis has confirmed that the surface tension of liquid Ni–Yb alloy is less than that of the first two alloys (Table 2).

### 3.2 Calculation results and analysis of viscosity and surface activation energy

The viscosity is calculated according to Eq. (18). Figure 2 shows the relationship between the viscosity of the system and the temperature with three different solute elements.

Fitting result of viscosity according to Eq. (18):

$$\eta_{\text{Ni-15\%Co}} = 0.4960 \times \exp\left(\frac{28476}{RT}\right), \quad (29)$$

$$\eta_{\text{Ni-15\%Cu}} = 0.8843 \times \exp\left(\frac{19876}{RT}\right), \quad (30)$$

$$\eta_{\text{Ni-15\%Yb}} = 0.8237 \times \exp\left(\frac{16791}{RT}\right). \quad (31)$$

It can be seen that the viscosity of liquid Ni-15%X (Co, Cu, Yb) alloys decreases exponentially with increasing temperature, which is consistent with the actual situation. It is well understood that the viscosity changes with temperature: the higher the temperature, the bigger is the spacing between atoms, so the atoms in the liquid system have a larger movement space. Similar to the surface tension, the viscosity is also affected by the melt composition and temperature.

### 3.3 Calculation results and analysis diffusion coefficient and diffusion activation energy

The diffusion coefficient is calculated according to Eq. (19). Figure 3 shows the relationship between the diffusion coefficient of liquid Ni-15%X (Cu, Co, Yb) alloys and temperature.

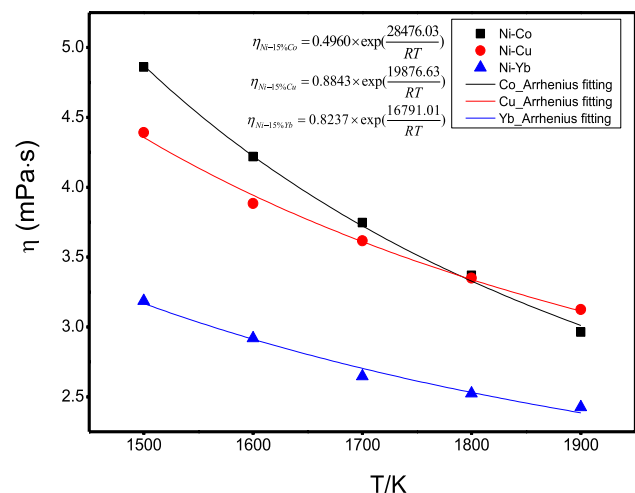
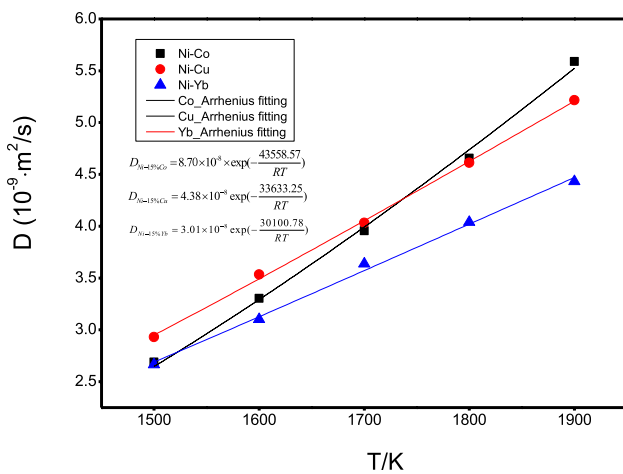


Fig. 2 The relationship between the viscosity of liquid Ni-15%X (Co, Cu, Yb) alloys with temperature



**Fig. 3** The relationship between the diffusion coefficient of liquid Ni-15%X (Cu, Co, Yb) alloys with temperature

Obviously, the diffusion coefficient has the opposite trend with viscosity. The Stokes (Sutherland)–Einstein formula establishes the following relationship between viscosity and solute diffusion coefficient:

$$D = \frac{kT}{a\pi r\eta} \tag{32}$$

Among them,  $r$  is the characteristic particle radius. For liquid metal, its size can be treated as atomic radius and  $a$  is constant. When the solute atom radius has slight difference from the solvent atom,  $a = 4$ , if not,  $a = 6$ . Therefore,  $a$  is 4 in Ni–Co and Ni–Cu systems, and  $a$  is 6 in the Ni–Yb system. The diffusion coefficients of liquid Ni-15%X (Co, Cu, Yb) alloys is obtained by fitting from 1500~1900 K.

Diffusion coefficient of Co:

$$D_{Ni-15\%Co} = 8.70 \times 10^{-8} \times \exp\left(-\frac{43558}{RT}\right) \tag{33}$$

Diffusion coefficient of Cu:

$$D_{Ni-15\%Cu} = 4.38 \times 10^{-8} \times \exp\left(-\frac{33633}{RT}\right) \tag{34}$$

Diffusion coefficient of Yb:

$$D_{Ni-15\%Yb} = 3.01 \times 10^{-8} \times \exp\left(-\frac{30100}{RT}\right) \tag{35}$$

As shown above, the diffusion coefficient of Co atoms in Ni-15% Co alloy melt is  $8.70 \times 10^{-8} \text{ m}^2/\text{s}$ , and the apparent activation energy is  $4.36 \times 10^4 \text{ J mol}^{-1}$ ; the diffusion coefficient of Cu atoms in Ni-15% Cu alloy melt is  $4.38 \times 10^{-8} \text{ m}^2/\text{s}$ , and the apparent activation energy is  $3.36 \times 10^4 \text{ J mol}^{-1}$ ; the diffusion coefficient of Yb atoms in Ni-15%Yb alloy melt is  $3.01 \times 10^{-8} \text{ m}^2/\text{s}$ , and the apparent

activation energy is  $3.01 \times 10^4 \text{ J mol}^{-1}$ . Under the same component, the diffusion coefficient increases exponentially with the increase of temperature.

### 3.4 Simulation results of average energy of atoms in liquid Ni-15% (Co, Cu, Yb) alloys at different temperatures

Figures 4 and 5 show the simulation results of the system energy of liquid Ni-15% X (Co, Cu, Yb) alloys in five different temperature states. After the quadratic function fitting of these simulated results from 1500~2000 K, the function relationship between energy and temperature is obtained.

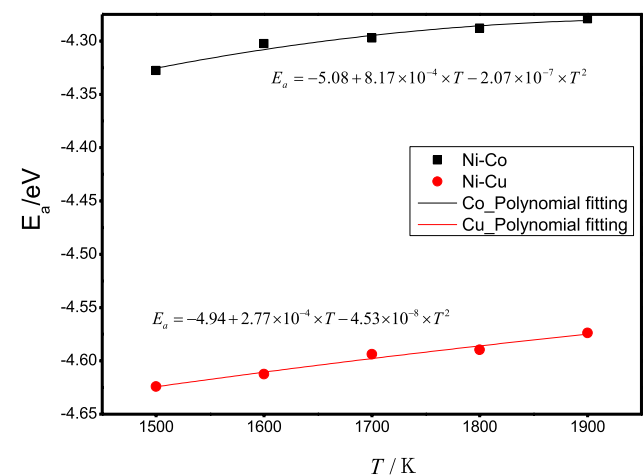


**Fig. 4** Simulation results of average energy of atoms in liquid Ni-15% (Co, Cu) alloys at different temperature

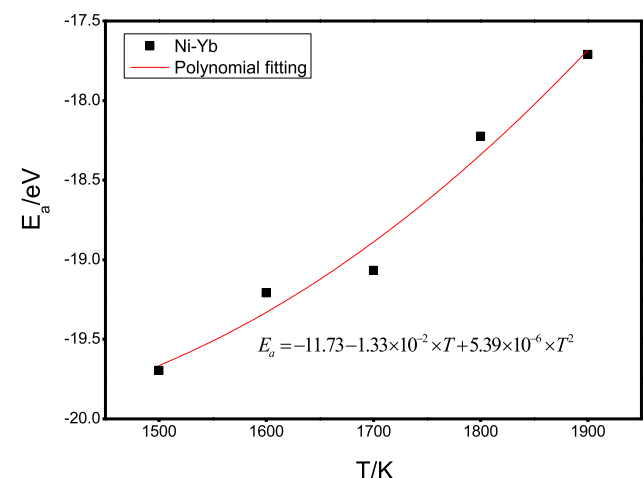


**Fig. 5** Simulation results of average energy of atoms in liquid Ni-15%Yb alloy at different temperatures

**Table 1** The model parameters of EAM for Ni, Cu and Co

The model parameters						
Atom type	$E_c$	$f_e$	$\phi_e$	$\alpha$	$\beta$	$\gamma$
Ni	4.45	0.41	0.74	4.98	6.41	8.86
Cu	3.54	0.30	0.59	5.09	5.85	8.00
Co	4.43	0.49	0.33	5.52	5.26	21.0

**Table 2** The model parameters of EAM for Yb

The model parameters							
Atom type	$F_o$	$f_e$	$e$	$N$	$\alpha$	$\beta$	$\gamma$
Yb	0.902 7	0.100 9	0.090 8	0.788	5.775	4.753 4	6

$$\text{Ni-15\%Co} : E_a = -5.08 + 8.17 \times 10^{-4} \times T - 2.07 \times 10^{-7} \times T^2 \text{ eV}, \quad (36)$$

$$\text{Ni-15\%Cu} : E_a = -4.94 + 2.77 \times 10^{-4} \times T - 4.53 \times 10^{-8} \times T^2 \text{ eV}, \quad (37)$$

$$\text{Ni-15\%Yb} : E_a = -11.73 + 1.33 \times 10^{-2} \times T + 5.39 \times 10^{-6} \times T^2 \text{ eV}. \quad (38)$$

Hence, specific heat and specific heat temperature coefficient of Ni-15% Co alloy melt at the melting point temperature can be obtained from the simulation.

$$C_{P_0} = 37.69 \text{ J} \cdot \text{mol}^{-1} \cdot \text{K}^{-1}, \quad (39)$$

$$\frac{dC_P}{dT} = -3.99 \times 10^{-2} \text{ J} \cdot \text{mol}^{-1} \cdot \text{K}^{-2}. \quad (40)$$

The relationship between specific heat and temperature of the Ni-15% Co alloy is

$$C_P = 37.69 - 3.99 \times 10^{-2}(T - T_m) \text{ J} \cdot \text{mol}^{-1}. \quad (41)$$

The same analysis of simulated data for Ni-15%Cu and Ni-15%Yb alloys is available.

$$C_P = 13.98 - 0.87 \times 10^{-2}(T - T_m) \text{ J} \cdot \text{mol}^{-1}, \quad (42)$$

$$C_P = 171.57 - 1.0383(T - T_m) \text{ J} \cdot \text{mol}^{-1}. \quad (43)$$

Compared with pure metal, the data of specific heat of Ni-15%X (Co, Cu) are within a reasonable range. There is a huge difference between Ni-15%X (Co, Cu) and Ni-15%Yb in terms of specific heat; however, the experimental data in this area are lacking and further research needs to be carried on.

## 4 Conclusion

In summary, we use the embedded-atom method to simulate the surface tension of liquid Ni-15%X (Co, Cu, Yb) alloys in the temperature range of 1500~1900 K, and deduce the viscosity and apparent activation energy, diffusion coefficient and diffusion activation energy of the system. The simulated data provide a feasible analysis of the thermodynamic behavior in the liquid nonequilibrium state. The calculation time shows a quadratic relationship as the number of particles increases; hence, only 864 atoms are taken for simulation. The size of the system is much smaller than the real macrostructure. Moreover, the MC steps of 100,000 are not enough for the number of steps required to achieve a true equilibrium. Therefore, there will be some errors in the simulation results. However, this paper mainly verifies the feasibility of the theoretical model in the study of the thermophysical properties of binary alloys. It is good to achieve such an acceptable accuracy in a limited time. In later studies, we will study the multicomponent alloy system, by increasing the number of atoms and the number of Monte Carlo steps to make the system closer to the actual results, and then provide more credible theoretical data for the study of liquid alloys.

**Acknowledgements** This work was supported by Aviation Science Foundation (under project No. 2018ZF53).

## References

1. T. Ohata, Y. Nakamura, T. Katayama, *J Mater Process Technol* **80**, 635 (1998)
2. M. Zhang, S. Zhang, L. Zheng, *Comput Fluids* **59**, 61 (2012)
3. L. Rougier, A. Jacot, *Acta Mater* **61**, 6396 (2013)
4. H. Zargamezhad, A. Dolati, *Electrochim Acta* **236**, 1 (2017)
5. H. Zhang, K. Zhang, *J Alloy Compd* **623**, 374 (2015)

6. K. Bai, F.L. Ng, *J Alloy Compd* **699**, 1084 (2017)
7. H. Deng, W. Hu, X. Shu, *Surf Sci* **517**, 177 (2002)
8. S.A. Mirkhani, F. Gharagheizi, *J Mol Liq* **179**, 78 (2013)
9. A. Dogan, Hüseyin Arslan. *Phil Mag* **98**, 37 (2018)
10. A. Dogan, Hüseyin Arslan. *Phil Mag* **99**, 267 (2019)
11. W.J. Yao, R.N. Yang, N. Wang, *J Alloy Compd* **627**, 410 (2015)
12. D. Giuranno, S. Amore, *J Mater Sci* **50**, 3763 (2015)
13. A. Dogan, Hüseyin Arslan. *Phil Mag* **96**, 459 (2016)
14. F.M. Menger, S.A.A. Rizvi, *Langmuir* **27**, 13975 (2011)
15. C.L. Kelchner, S.J. Plimpton, J.C. Hamilton, *Phys Rev B* **58**, 110 (1998)
16. M.S. Daw, M.I. Baskes, *Phys Rev B: Condens Matter* **29**, 643 (1984)
17. M.S. Daw, M.I. Baskes, *Phys Rev Lett* **50**, 1285 (1983)
18. R.A. Johnson, *Phys Rev B* **39**, 12554 (1989)
19. J.H. Rose, P. Vinet, J. Ferrante, *J Phys C: Solid State Phys* **19**, 467 (1986)
20. J.K. Baria, A.R. Jani, *Phys B* **405**, 2065 (2010)
21. W.J. Yao, X.J. Han, M. Chen, B. Wei, Z.Y. Guo, *J Phys Condens Matter* **14**, 7479 (2002)
22. I. Egry, *Scr Metall Mater* **28**, 1273 (1993)
23. T. Gaskell, *J Non-Cryst Solids* **61**, 913 (1984)
24. G. Wilde, G.P. Görler, R. Willnecker, *Appl Phys Lett* **68**, 2 (1996)
25. Y. Tsuchiya, *J Phys: Condens Matter* **3**, 3 (1991)
26. G. Wilde, *J Non-Cryst Solids* **307**, 853 (2002)

**Publisher's Note** Springer Nature remains neutral with regard to jurisdictional claims in published maps and institutional affiliations.